

Journal of Materials Chemistry A

Accepted Manuscript



This is an *Accepted Manuscript*, which has been through the Royal Society of Chemistry peer review process and has been accepted for publication.

Accepted Manuscripts are published online shortly after acceptance, before technical editing, formatting and proof reading. Using this free service, authors can make their results available to the community, in citable form, before we publish the edited article. We will replace this *Accepted Manuscript* with the edited and formatted *Advance Article* as soon as it is available.

You can find more information about *Accepted Manuscripts* in the [Information for Authors](#).

Please note that technical editing may introduce minor changes to the text and/or graphics, which may alter content. The journal's standard [Terms & Conditions](#) and the [Ethical guidelines](#) still apply. In no event shall the Royal Society of Chemistry be held responsible for any errors or omissions in this *Accepted Manuscript* or any consequences arising from the use of any information it contains.

COMMUNICATION

Three dimensional hierarchical pompon-like Co_3O_4 porous spheres for high-performance lithium-ion batteries

Cite this: DOI: 10.1039/x0xx00000x

Received 00th,
Accepted 00thWenjun Hao,^a Shimou Chen,^b Yingjun Cai,^b Lan Zhang,^b Zengxi Li^{*a} and Suojiang Zhang^{*b}

DOI: 10.1039/x0xx00000x

www.rsc.org/

Three dimensional hierarchical pompon-like Co_3O_4 porous spheres were synthesized by a hydrothermal method. It was found that crystal-splitting mechanism plays a key role in the formation of these pompon-like structures. When tested as anode materials in lithium ion batteries (LIBs), they exerted higher specific capacity and better cycle performance than those of Co_3O_4 nanoparticles and nanowires.

Lithium-ion batteries (LIBs) have been regarded as an excellent power source for energy conversion and storage technology due to their advantages of high energy density, long lifespan, no memory effect and environmental benignity.¹⁻³ As one of the key components of LIBs, electrode material dominates the electrochemical properties and performances of the device. Numerous efforts have been made to develop new electrode materials with specific morphology and composition to enhance the properties of the LIBs, such as nanoparticles,⁴ nanowires,⁵⁻⁷ nanosheets,⁸ nanotubes,⁹ etc.

Recently, the anode electrodes made of transition-metal oxides have attracted much attention owing to their much higher capacity than that of graphite ($378 \text{ mAh}\cdot\text{g}^{-1}$). Among the transition-metal oxides, Co_3O_4 received special interests for its high theoretical capacity ($890 \text{ mAh}\cdot\text{g}^{-1}$).¹⁰ However, the poor cycling stability owing to the large volume changes during the repeated Li^+ intercalation/

deintercalation processes hinders its practical application.¹¹ A variety of approaches have been tried to prepare nanometer-scale Co_3O_4 with diverse morphologies to restrain the large volume changes.¹² Among them, fabrication of Co_3O_4 nanomaterials with three dimensional (3D) hierarchical structures has been considered as one of the most promising approaches. Theoretically, the 3D-hierarchical structures facilitate ion transport by providing large surface area which enables more accesses for more Li ions, as well as shorten the diffusion pathway of the Li ions. Furthermore, the large cavities of the 3D frameworks can alleviate volume strain and stabilize the structures during the intercalation-deintercalation processes.¹³⁻¹⁷ However, most of the present 3D hierarchical structures of Co_3O_4 were multi-step synthesized and costly due to the use of templates.^{17,18}

Herein, we report a new approach for preparing Co_3O_4 nanoparticles, nanowires and 3D pompon-like hierarchical Co_3O_4 structures in a controlled manner *via* hydrothermal method. These structures exhibited different electrochemical performances when they are used in lithium ion batteries (LIBs), in which 3D hierarchical structure is better than those nanowires and nanoparticles. In addition, we also investigated the growth mechanism of 3D hierarchical Co_3O_4 by controlling the hydrothermal reaction time, and found that the crystal splitting plays an important role in the formation of the hierarchical spheres.

The Co_3O_4 was obtained by a hydrothermal method in the presence of Cobalt nitrate hexahydrate ($\text{Co}(\text{NO}_3)_2\cdot 6\text{H}_2\text{O}$), urea ($\text{CO}(\text{NH}_2)_2$) and water, followed by a calcination treatment. Fig. 1 shows three kinds of Co_3O_4 with different morphologies obtained by changing the molar ratio (M.R.) of $\text{Co}(\text{NO}_3)_2\cdot 6\text{H}_2\text{O}$ and urea. It was found that the molar ratio, hydrothermal reaction temperature and the concentration of the Co^{2+} affect the formation of the final Co_3O_4 structures. By optimizing the hydrothermal reaction conditions, we obtained the uniform nanoparticles, nanowires and 3D pompon-like Co_3O_4 spheres, respectively (Fig. 1). The 3D pompon-like spheres with a diameter ranging from $8 \mu\text{m}$ to $20 \mu\text{m}$ (Fig. 1c) were composed of lots of nanowires gathered a ring in the centre and fanned out to the outside (see ESI, Fig. S1). The pompon-like feature of the Co_3O_4 spheres was also confirmed by TEM. At low magnification, the TEM image (Fig. 2a) demonstrated that bundles

^a School of Chemistry and Chemical Engineering, University of Chinese Academy of Sciences (UCAS), Beijing 100049, PR China. E-mail: zqli@home.ipe.ac.cn

^b Beijing Key Laboratory of Ionic Liquids Clean Process, Key Laboratory of Green Process and Engineering, Institute of Process Engineering (IPE), Chinese Academy of Sciences (CAS), Beijing 100190, PR China. E-mail: sjzhang@home.ipe.ac.cn

† Electronic Supplementary Information (ESI) available: Experimental part, SEM images, XRD patterns and Impedance spectra for all three kinds of Co_3O_4 materials.

See DOI: 10.1039/c000000x/

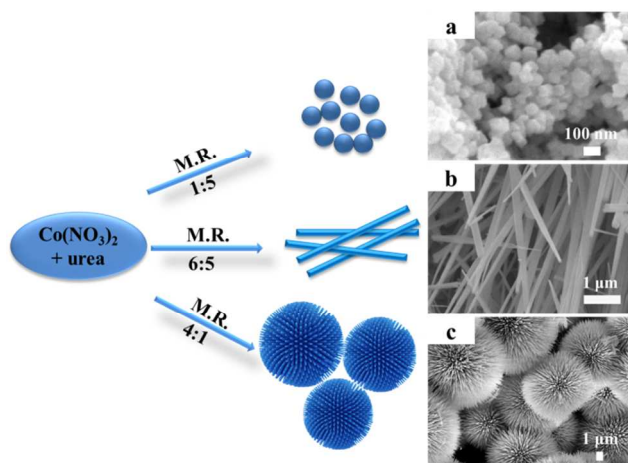


Fig. 1 Low-magnification SEM images of three kinds of Co_3O_4 with different morphologies: a) nanoparticles; b) nanowires; c) 3D pompon-like porous spheres.

of nanowires were embodied in the Co_3O_4 structures. Fig. 2b shows the HR-TEM observation of the composed nanowires, which clearly indicates the crystal structure of the materials. The measured lattice spacings of 0.286 nm and 0.244 nm are in good agreement with the lattice spacings of the [220] and [311] planes of Co_3O_4 , respectively (Fig. 2b). In addition, the corresponding SAED pattern (inset in Fig. 2b) shows a polycrystalline nature of the hierarchical structure, indicating that the nanowires of the pompon-like Co_3O_4 spheres are randomly orientated.

The X-ray powder diffraction (XRD) pattern shows seven diffraction peaks, which perfectly matched to the cubic Co_3O_4 (Fig. 2c, Fig. S2). We further evaluated the porous structure of the 3D pompon-like Co_3O_4 by N_2 physical adsorption instrument based on BET method. Fig. 2d shows the adsorption-desorption isotherm and the Barrett-Joyner-Halenda (BJH) pore-size-distribution plot. According to the IUPAC classification, the shape of hysteresis loop was ascribed to Type H3,^{18,19} meaning the existence of affluent pores

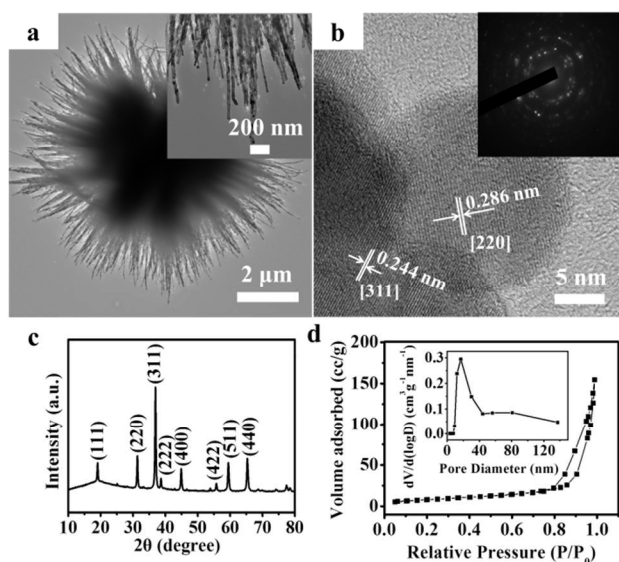


Fig. 2 a) TEM image of the 3D hierarchical pompon-like Co_3O_4 ; b) HR-TEM image and SAED pattern (inset) of Co_3O_4 nanowires at the tip of the 3D pompon-like spheres; c) XRD pattern of 3D pompon-like Co_3O_4 ; d) Nitrogen-adsorption-desorption isotherm and pore-size-distribution curve (inset) of the pompon-like Co_3O_4 .

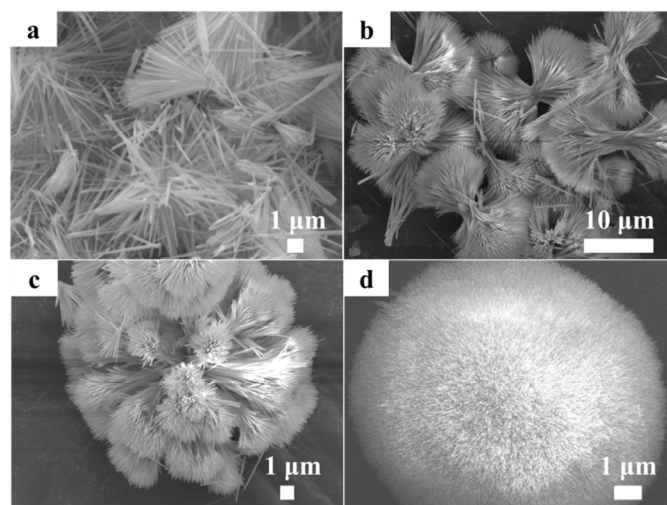


Fig. 3 SEM images of the Co_3O_4 precursors synthesized at 160 °C for different hydrothermal reaction time: a) 20 min; b) 40 min; c) 1 h; d) >6 h.

with diameter ranging from 15 to 25 nm in diameter. The vast majority of the pores' sizes were around 17 nm in diameter (pore volume: $0.245 \text{ cm}^3 \cdot \text{g}^{-1}$). The surface area (BET) of the 3D pompon-like sphere was $29.5 \text{ m}^2 \cdot \text{g}^{-1}$.

Formation process of the 3D pompon-like Co_3O_4 products was further investigated at different reaction stages to find a clue for the possible growth mechanisms. Fig. 3 shows the different morphologies of the precursor changed over hydrothermal reaction time. After the initial reaction time most of the nanowire precursors gathered into dumbbell-shaped hemispheres (Fig. 3b). With increasing the hydrothermal reaction time to 1 h, more nanowires were produced with plumper microspheres to form well-organized flower-like microspheres (Fig. 3c), whose orientations gradually deviate from those of the initial crystal, indicating these microspheres may be formed by the splitting crystal growth mechanism.^{14,20-23} Finally, these assemblies transformed into uniform pompon-like Co_3O_4 after continuous hydrothermal reacting for longer than 6 h (Fig. 3d). The resulting products showed three remarkable structural characteristics: unusual pompon-like, hierarchical and porous. Our results support the idea that both the assembly of urea and its effects on the crystal splitting play important roles in the formation of the 3D pompon-like structures, as reported by Wang, et al.,¹⁸ small organic molecules as the complex agents may densely cover the surface of some exposed Co_3O_4 facets, then regulate the nanocrystal fusion or growth towards some specific direction. Thus, nanowire bundles with fan-shaped structures were formed (Fig. 3a). On the other hand, similar to the reported Co_3O_4 nanowires assembly behaviour,^{19,24,25} its 1D nanowires precursor can easily grow into sheaf-like bundles according to a crystal-splitting mechanism.²⁰⁻²³ In our experiments, the urea act not only as a reactant to regulate the growth of the nanowire precursor, but also as a surfactant to bedeck the growth of the nanowire along one direction and induce them gathered a ring in the centre and fanned out (Fig. 3b-3d). It is worth noting that the final products show very high stability, as the calcinations of the structures have no impact on the morphology of the Co_3O_4 (Fig. S3). The 3D pompon-like morphologies maintained very well after calcinations.

The electrochemical performances of the three types of calcined Co_3O_4 with different morphologies (nanoparticles, nanowires and 3D pompon-like Co_3O_4 spheres) were investigated by configuring them as the CR2032 coin cell in the voltage range between 0.01 and 3.2 V. Fig. 4a shows the discharge-charge capacities versus voltage of the

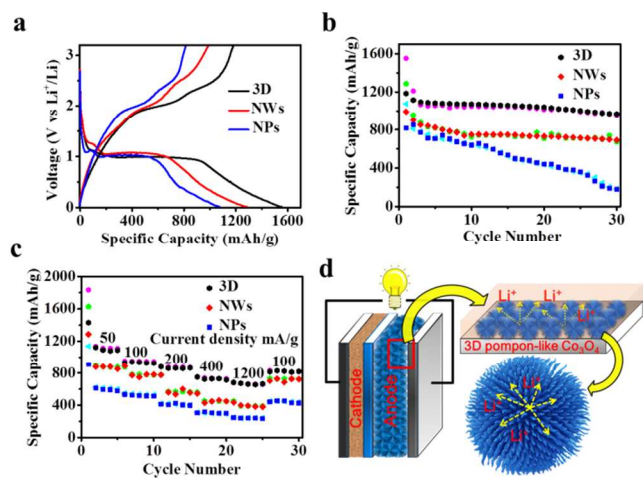


Fig. 4 Electrochemical characterizations: a) Cycling performance of the three kinds of Co_3O_4 at a current density of $50 \text{ mA}\cdot\text{g}^{-1}$; b) First-cycle discharge-charge curves for the three kinds of Co_3O_4 materials (3D: 3D pompon-like Co_3O_4 spheres; NWs: Nanowires; NPs: Nanoparticles) at a current density of $50 \text{ mA}\cdot\text{g}^{-1}$; c) Rate performance of the three kinds of Co_3O_4 at different current densities; d) Schematic illustrations of the lithium ion battery with pompon-like Co_3O_4 as anode material.

three kinds of materials at the first cycle. A clear potential plateau was showed in the discharge curves at about 1.0 V vs Li^+/Li . Fig. 4b is the charge-discharge capacities versus cycle numbers of the three different morphologies of Co_3O_4 at a current density of $50 \text{ mA}\cdot\text{g}^{-1}$. The initial discharge capacities of the three samples are 1552, 1285, 1074 $\text{mAh}\cdot\text{g}^{-1}$, respectively, all of them are higher than the theoretical capacity ($890 \text{ mAh}\cdot\text{g}^{-1}$), which could be attributed to the formation of a solid electrolyte interface (SEI) and the interaction with the electrolyte.²⁶⁻²⁸ It was clearly found that 3D pompon-like Co_3O_4 showed much better lithium storage capacity and cycling performance than the other two samples. To investigate the rate performance of the pompon-like Co_3O_4 , the batteries were cycled at various current densities of 50, 100, 200, 400 and $1200 \text{ mA}\cdot\text{g}^{-1}$ in the voltage range of 0.01-3.2 V (Fig. 4c). The 3D pompon-like Co_3O_4 spheres maintained high capacity of $780 \text{ mAh}\cdot\text{g}^{-1}$ when the current density was increased to $400 \text{ mA}\cdot\text{g}^{-1}$. Even at a much larger current density of $1200 \text{ mA}\cdot\text{g}^{-1}$, our products still show a considerable reversible capacity of $650 \text{ mAh}\cdot\text{g}^{-1}$. Both the rate and cyclic performance of the 3D pompon-like Co_3O_4 are better than those Co_3O_4 electrode materials with the structure of nanowires and nanoparticles. It should be mentioned that the capacities of the 3D pompon-like Co_3O_4 after the second cycle are still higher than the theoretical capacity ($890 \text{ mAh}\cdot\text{g}^{-1}$) when tested at a lower current density ($50-100 \text{ mA}\cdot\text{g}^{-1}$). Besides the redox reaction, the extra capacity may be ascribed to a thicker SEI film or interfacial lithium storage mechanisms.²⁹ Fig. 4d shows the illustrations of the possible Li^+ transfer mode within pompon-like Co_3O_4 anode material.

The excellent electrochemical performance of the 3D pompon-like Co_3O_4 is believed to originate from its unique structural features. Firstly, similar to researches on hollow structured anodes, the void space in our pompon-like spheres can effectively buffer the volume changes during lithium intercalation-deintercalation, hence alleviate the pulverization of the electrode and improve the cycling stability. To check this hypothesis, the electrode at the fully lithiated states after 30 cycles was separated from the LIB, after washed with large amount of DMF and full dried in vacuum for more than 24 h, then it was characterized by SEM. As shown in Fig. 5, the electrode material maintains the pompon-like shape after 30 cycles; it reveals excellent structural stability of Co_3O_4 , which is one of the main

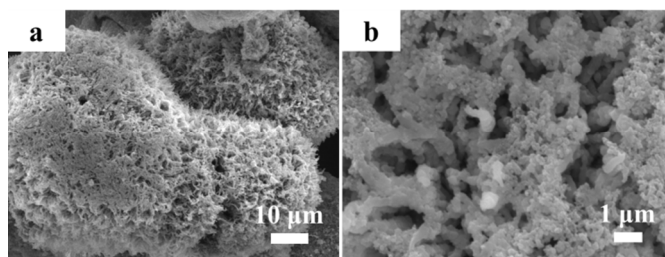


Fig. 5 a,b) The SEM images of the 3D pompon-like Co_3O_4 tested as lithium-ion batteries anode materials after 30 cycles.

reasons for superior performance of pompon-like structure. However, it is also worth noting that there is obviously a morphology change of the bundles of nanowires in the 3D pompon-like structure. The twisting bundles may due to the volume-changing during the lithium ions intercalation/deintercalation processes.^{30,31} Secondly, the increasing specific capacity for pompon-like sphere Co_3O_4 electrodes can be ascribed to the reversible growth of a polymeric gel-like film resulting from kinetically activated electrolyte degradation.³² The plenty of nanowires in pompon-like sphere and the high density active interfaces in hierarchical structures can facilitate the reaction of Li with electrolyte. Fig. S4 shows the impedance of all three kinds of electrodes before cycling. All of the impedance spectra have similar characteristics: a depressed semicircle at high-medium frequency and an inclined line at low frequency which is in good accordance with previously reported impedance spectra for Co_3O_4 .³³ The inclined line is attributed to the lithium diffusion impedance. Moreover, the depressed semicircles are ascribed to charge impedance.³⁴ It indicated that the 3D porous structure has benefited improving the conductivity of the electrode. Fig. S5 showed the impedance spectra of three kinds of Co_3O_4 at the 5th cycle. It is obviously showed that there is another smaller semicircle in each impedance spectra which is attributed to the formation of SEI films. It is noteworthy that the smaller semicircle of the 3D pompon-like Co_3O_4 electrode is larger than the other two electrodes. This phenomenon is owing to the formation of a much thicker SEI film which may leads to the capacities of 3D pompon-like Co_3O_4 higher than theoretical capacity.²⁹ Thirdly, the 3D porous structures in pompon-like sphere not only render a very short transport length for Li^+ during intercalation/deintercalation, but also bring a 3D transport direction of the lithium, favouring a high rate performance (Fig. 4d).

In summary, we have successfully demonstrated a new and effective hydrothermal method to fabricate an ordered nanostructure of 3D pompon-like hierarchical Co_3O_4 . The 3D structure composed by plenty of nanowires gathered a ring in the centre and fanned out via a special self-assembly fashion. Due to the unique structural features, such pompon-like spheres exhibit superior electrochemical performance when served as the anode material for LIBs. The unusual 3D hierarchical structures can not only offer stable structure for the volume change but also provide a short ion transport pathway during cycling. The results suggested we can design and fabricate other transition metal oxide materials with this unique hierarchical structure, which may further improve their performance in LIBs, electrochemical capacitors or sensors.

Acknowledgement

† This work was supported by National Natural Science Foundation of China (No. 21276257, 21210006) and Beijing Natural Science

Foundation (2132054) and “Strategic Priority Research Program” of the Chinese Academy of Sciences (Grant No. XDA09010103)

References

- 1 S. Y. Zheng, Y. Chen, Y. H. Xu, F. Yi, Y. J. Zhu, Y. H. Liu, J. H. Yang and C. S. Wang, *ACS Nano*, 2013, **7**, 10995-11003.
- 2 J. B. Goodenough and Y. Kim, *Chem. Mater.*, 2010, **22**, 587-603.
- 3 B. Dunn, H. Kamath and J. M. Tarascon, *Science*, 2011, **334**, 928-935.
- 4 C. Z. Yuan, L. Yang, L. R. Hou, L. F. Shen, F. Zhang, D. K. Li and X. Q. Zhang, *J. Mater. Chem.*, 2011, **21**, 18183-18185.
- 5 B. Wang, T. Zhu, H. B. Wu, R. Xu, J. S. Chen and X. W. Lou, *Nanoscale*, 2012, **4**, 2145-2149.
- 6 X. H. Xia, J. P. Tu, Y. Q. Zhang, Y. J. Mai, X. L. Wang, C. D. Gu and X. B. Zhao, *RSC Adv.*, 2012, **2**, 1835-1841.
- 7 Y. Y. Gao, S. L. Chen, D. X. Cao, G. L. Wang and J. L. Yin, *J. Power Sources*, 2010, **195**, 1757-1760.
- 8 Y. Q. Fan, H. B. Shao, J. M. Wang, L. Liu, J. Q. Zhang and C. N. Cao, *Chem. Commun.*, 2011, **47**, 3469-3471.
- 9 X. H. Xia, J. P. Tu, Y. J. Mai, X. L. Wang, C. D. Gu and X. B. Zhao, *J. Mater. Chem.*, 2011, **21**, 9319-9325.
- 10 R. H. Wang, C. H. Xu, J. Sun, Y. Q. Liu, L. Gao and C. C. Lin, *Nanoscale*, 2013, **5**, 6960-6967.
- 11 X. L. Huang, X. Zhao, Z. L. Wang, L. M. Wang and X. B. Zhang, *J. Mater. Chem.*, 2012, **22**, 3764-3769.
- 12 D. W. Wang, F. Li, M. Liu, G. Q. Lu and H. M. Cheng, *Angew. Chem. Int. Ed.*, 2008, **47**, 373-376.
- 13 X. Y. Li, X. L. Huang, D. P. Liu, X. Wang, S. Y. Song, L. Zhou and H. J. Zhang, *J. Phys. Chem. C*, 2011, **115**, 21567-21573.
- 14 F. Wang, W. Z. Tao, M. S. Zhao, M. W. Xu, S. C. Yang, Z. B. Sun, L. Q. Wang and X. P. Song, *J. Alloys Compd.*, 2011, **509**, 9798-9803.
- 15 X. Y. Yu, R. X. Xu, C. Gao, T. Luo, Y. Jia, J. H. Liu and X. J. Huang, *ACS Appl. Mater. Interfaces*, 2012, **4**, 1954-1962.
- 16 A. M. Cao, J. S. Hu and L. J. Wan, *Sci. China Chem.*, 2012, **55**, 2249-2256.
- 17 Y. H. Xiao, S. J. Liu, F. Li, A. Q. Zhang, J. H. Zhao, S. M. Fang and D. Z. Jia, *Adv. Funct. Mater.*, 2012, **22**, 4051-4058.
- 18 D. Q. Liu, X. Wang, X. B. Wang, W. Tian, Y. Bando and D. Golberg, *Sci. Rep.*, 2013, **3**, 2543-2548.
- 19 M. Fialkowski, K. J. M. Bishop, R. Klajn, S. K. Smoukov, C. J. Campbell and B. A. Grzybowski, *J. Phys. Chem. B.*, 2006, **110**, 2482-2496.
- 20 S. L. Cha, K. H. Hwang, Y. H. Kim, M. J. Yun, S. H. Seo, Y. J. Shin, J. H. Moon and D. Y. Lee, *Nanoscale*, 2013, **5**, 753-758.
- 21 L. X. Yang, Y. B. Ding, S. L. Luo, Y. Luo, F. Deng and Y. Li, *Semi. Sci. Technol.*, 2013, **28**, 035005.
- 22 X. F. Shen and X. P. Yan, *Angew. Chem. Int. Ed.*, 2007, **46**, 7659-7963.
- 23 L. F. Chen, J. C. Hu, R. Richards, S. Prikhodko and S. Kodambaka, *Nanoscale*, 2010, **2**, 1657-1660.
- 24 M. Grzelczak, J. Vermant, E. M. Furst and L. M. Liz-Marzan, *ACS Nano*, 2010, **4**, 3591-3605.
- 25 B. A. Grzybowski, C. E. Wilmer, J. Kim, K. P. Browne and K. J. M. Bishop, *Soft Matter*, 2009, **5**, 1110-1128.
- 26 K. T. Nam, D. W. Kim, P. J. Yoo, C. Y. Chiang, N. Meethong, P. T. Hammond, Y. M. Chiang and A. M. Belcher, *Science*, 2006, **312**, 885-888.
- 27 P. Poizat, S. Laruelle, S. Grugeon, L. Dupont and J. M. Tarascon, *Nature*, 2000, **407**, 496-499.
- 28 X. Wang, H. Guan, S. M. Chen, H. Q. Li, T. Y. Zhai, D. M. Tang and Y. Bando, *Chem. Commun.*, 2011, **47**, 12280-12282.
- 29 J. Y. Wang, N. L. Yang, H. J. Tang, Z. H. Dong, Q. Jin, M. Yang, D. Kisailus, H. J. Zhao, Z. Y. Tang and D. Wang, *Angew. Chem. Int. Ed.*, 2013, **52**, 6417-6420.
- 30 Y. G. Li, B. Tan and Y. Y. Wu, *Nano Lett.*, 2008, **8**, 265-270.
- 31 C. C. Li, X. M. Yin, L. B. Chen, Q. H. Li and T. H. Wang, *Chem. Eur. J.*, 2010, **16**, 5215-5221.
- 32 X. H. Wang, X. W. Li, X. L. Sun, F. Li, Q. M. Liu, Q. Wang and D. He, *J. Mater. Chem.*, 2011, **21**, 3571-3573.
- 33 J. Chen, X. H. Xia, J. P. Tu, Q. Q. Xiong, Y. X. Yu, X. L. Wang and C. D. Gu, *J. Mater. Chem.*, 2012, **22**, 15056-15061.
- 34 X. L. Chen, K. Gerasopoulos, J. C. Guo, A. Brown, C. S. Wang, R. Ghodssi and J. N. Culver, *ACS Nano*, 2010, **4**, 5366-5372.